SPE
REPRINT
SERIES

No. 13
VOLUME II

GAS TECHNOLOGY

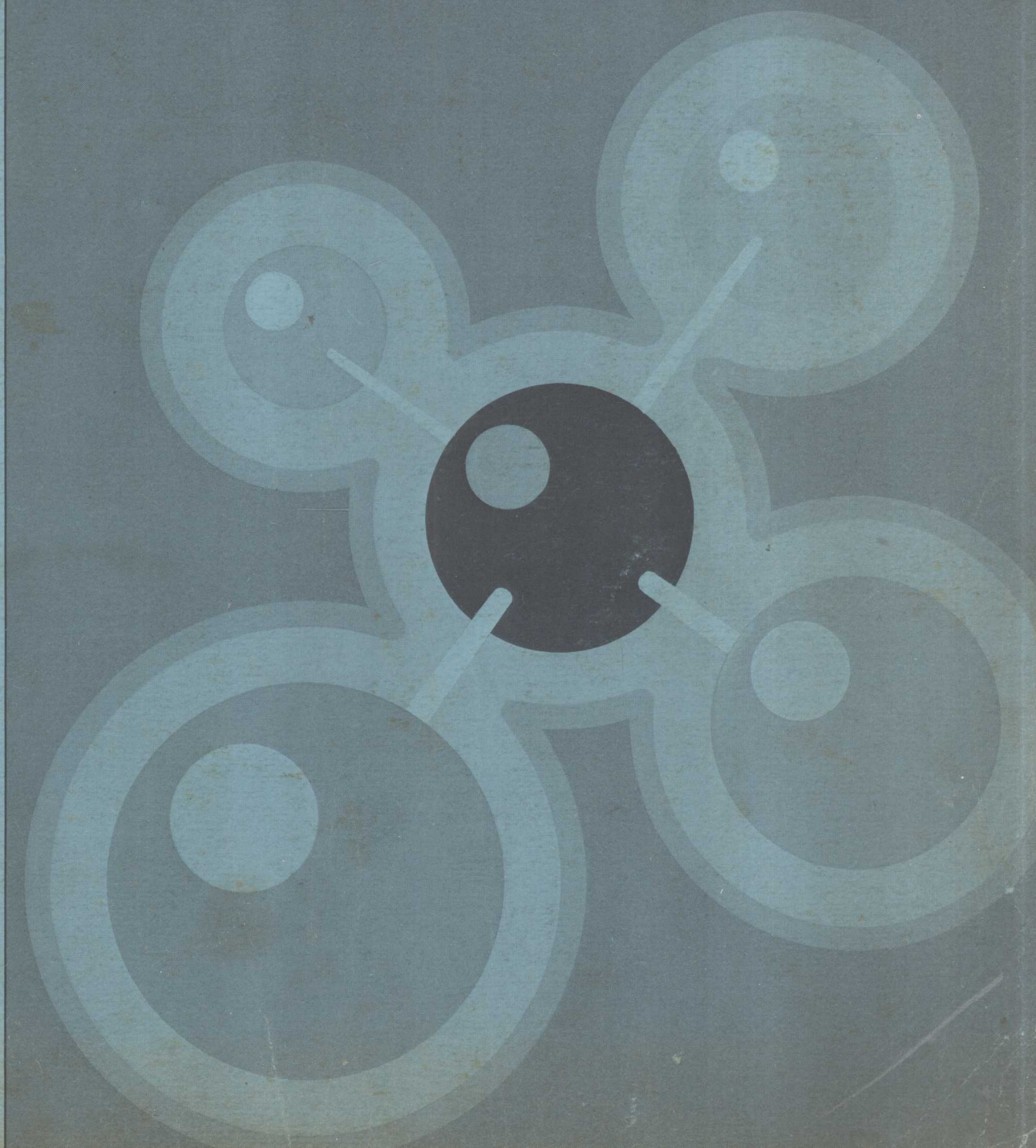

Published
by
the
Society
of
Petroleum
Engineers
of
AIME

SPE REPRINT SERIES NO. 13

Volume II

GAS TECHNOLOGY

1977 Edition

Published by the
Society of Petroleum Engineers of AIME
Dallas, Texas

PREFACE

Eighteen years have passed since the publication of the *Handbook of Natural Gas Engineering*, the premier work on the subject of gas technology. This has been a period not only of considerable increase in the value of gas but of substantial progress in the theory and practice of completing and producing gas wells and reservoirs.

The SPE Reprint Booklets on Gas Technology are intended to pick up where the *Handbook* left off, and bring to the reader the most up-to-date treatment of the subject.

The majority of the papers included in these volumes are application oriented. A few excellent papers are presented that treat the basic physics of gas flow and behavior.

The papers cover techniques suitable for both desk-calculator treatment and reservoir simulators. The simulation papers are presented, not with the idea of delving deeply into the formulation of models, but rather to show their practical application so that they might become a valuable tool to any engineer.

Space limits the number of papers that can be reprinted. The reader is directed to the bibliographies for the titles of many other fine papers, reprint booklets, and monographs on the subject of gas technology.

G. A. Mistrot

SPECIAL REPRINT COMMITTEE

TABLE OF CONTENTS

Part 4 — Gas Storage

Part 5 — Pipeline Gathering System and Multiphase Flow

Part 4 — Gas Storage

The first recorded attempt at underground storage was in Welland County, Ont., Canada, in 1915. This was followed in 1916 by Iroquois Gas Co.'s storage of gas in the Zoar field near Buffalo, N.Y., and in 1919 by Central Kentucky Natural Gas Co.'s use of the Menifee field for storage. These early projects were considered primarily as peak shaving devices, used to bolster supply when demands exceeded pipeline capacity. Later, as pipelines grew in length, the emphasis shifted to the use of storage as an aid in maintaining high pipeline load factors despite fluctuating markets, particularly the seasonal space heating load.

Initially, depleted gas fields were used exclusively. Later, as more storage was needed, companies began to utilize depleted oil fields as combination storage/secondary recovery projects (see, for instance, the paper "Secondary Oil Recovery and Gas Storage Operations in Reed City Oil Field" reprinted here). Storage in virgin aquifers was also tried and proved successful. Some of the special techniques that have been developed for use in aquifer storage are presented in "Case History of Aquifer Gas Storage Development in a Silurian Dolomite at Glasford, Illinois," "Control of Sand Production in the Underground Storage of Natural Gas," "Calculation of Gas Recovery Upon Ultimate Depletion of Aquifer Storage," and "Evaluating a Slightly Permeable Caprock in Aquifer Gas Storage." Natural gas has also been stored in leached and mine cavities, and has been contemplated in nuclear chimneys; for details see the bibliography. Of course, natural gas also can be liquefied and stored, but only storage in the gaseous state will be considered here.

The prime reference in the field of underground gas storage is *Underground Storage of Fluids* by D. L. Katz and K. H. Coats. The papers presented here represent a supplement to that work.

Many of the tools that have been developed for the study of producing fields also can be used to study gas storage. As an example, see "Use of Numerical Models to Develop and Operate Gas Reservoirs." However, certain unique problems arise from the severe demands placed on field deliverability (see "Maximizing Seasonal Withdrawals from Gas Storage Reservoirs"), and from the fact that storage reservoirs, unlike producing reservoirs, are cycled repeatedly. History can have an important effect on field performance (see "Evolution of Capillarity and Relative Permeability Hysteresis"), and the time available for tests is severely limited, leading to the use of techniques such as those presented in "Use of Injection-Falloff Tests To Evaluate Storage Reservoirs" and "Determining Average Reservoir Properties From Gathering-Line Transient Analysis for a Multiwell Reservoir."

Finally, because storage fields often represent a substantial investment, which must be able to perform at full capacity for many years, monitoring of their performance is important. "Monitoring Gas Storage Reservoirs" offers some insight into how this can be done.

Use of Numerical Models To Develop and Operate Gas Storage Reservoirs

JAMES H. HENDERSON
JUNIOR MEMBER AIME
JOHN R. DEMPSEY
MEMBER AIME
JAMES C. TYLER
JUNIOR MEMBER AIME

NORTHERN NATURAL GAS CO.
OMAHA, NEBR.

Abstract

Performance of gas storage reservoirs is affected by a combination of well placement and operational strategy. This paper illustrates the use of a two-dimensional, single phase dry gas reservoir simulator in the study of such a reservoir. Results are presented that illustrate the effects of well spacing and operational planning on the ability of a reservoir to meet certain requirements.

Introduction

In the design and operation of gas storage reservoirs, the placement of wells with respect to the most advantageous operational stratagem is of prime importance. The economic consequences of failing to give adequate attention to the effects of interference among wells can be great. In addition, the impact of operational stratagems on the desired performance of the reservoir must be considered. The level of season-end performance is subject to the effects of the method of operation during the season.

In this study, the placement of new wells in an existing dry gas storage reservoir is treated concurrently with the search for an operational stratagem that would permit the reservoir to meet certain withdrawal requirements. These investigations were carried out using a two-dimensional, single-phase reservoir simulator based on Eq. 1.

$$-\nabla \cdot \rho_g v_g + q_g = \phi S_g \frac{\partial \rho_g}{\partial t} \quad . \quad . \quad . \quad . \quad . \quad . \quad . \quad (1)$$

(The reservoir model is described in detail in the Appendix.) This study also illustrates one approach to the problem of extracting a workable reservoir description from meager data.

Definition of Problem

The object of the study was a nearly depleted dry gas Oriskany sand reservoir that had been converted to gas storage. In operation as a storage field, the main portion of the reservoir contained 41 wells and, under a given seasonal operational plan, was capable of delivering 140 MMcf/D on the last day of withdrawal. It was required that turnover of gas be increased and that the last-day capacity be upgraded to 300 MMcf/D. This was to be accomplished by drilling additional wells and adding compressor horsepower so that field gathering-line pressure could be lowered. Plans were made for extra compression and 38 new wells, so the problem reduced to one of correct well placement with the possibility that perhaps one or more wells could be eliminated from the plan and yet the required deliverability could be met.

Description of Reservoir

The computing grid was superimposed on the reservoir map as shown in Fig. 1. The block size was chosen as a compromise between computing speed and definition. Also shown in Fig. 1 are deliverability areas defined from observed performance of the wells. These areas are labeled in order of quality; i.e., Area 1 contains the wells with the highest deliverability and Area 6 contains those with the lowest. These area definitions show that the reservoir decreases in quality outward from a central zone. These data, along with gelogic interpretations, led to a contour map of gas-filled porosity that generally followed the same pattern. Values of porosity were entered on the grid at selected control points and a statistical regression technique was used to obtain values over the entire grid. Log picks indicated that a constant value of 7 ft for net pay thickness over the entire grid was reasonable.

Obtaining a representation of permeability posed some problems. Core data were available for one well and pressure vs injection/production data were recorded only on a cumulative reservoir basis. Thus, in the absence of individual well drawdown or buildup data, the only available means of obtaining a detailed reservoir description was through the use of deliverability curves for each well. Initial values of permeability were selected on the basis of flow capacity, and the regression routine was used to obtain values over the full grid, with the wells serving as control points.

Using constant pressure boundary conditions, we then set up the model to compute deliverability curves for each well. We computed three points on these curves during each pass, each time restoring the grid to initial pressure and using a different limiting pressure. To shift the computed curve so as to match the observed curve, we made hand adjustments to grid block values of permeability at wells. To smooth the entire grid, we used an arithmetic moving average procedure that held the values at these control points as constant. In some instances values of

Original manuscript received in Society of Petroleum Engineers office March 11, 1968. Revised manuscript received Oct. 3, 1968. Paper (SPE 2009) was presented at SPE Symposium on Numerical Simulation of Reservoir Performance held in Dallas, Tex., April 22-23, 1968.

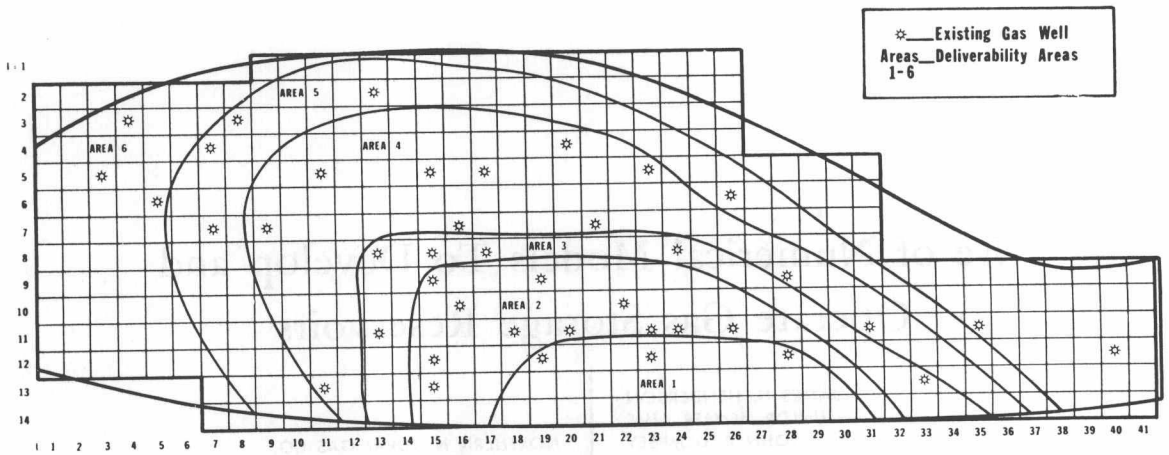

Fig. 1 — *Reservoir outline with computing grid.*

permeability in blocks adjacent to wells were entered by hand and also used as control points. The observed and simulated curves for a representative well are shown in Fig. 2. This plot shows that, for all wells, the calculated curve has a greater slope n as defined by the back pressure equation

$$q = c(\Delta p^2)^n \quad \ldots\ldots\ldots\ldots \quad (2)$$

than does the observed curve. This is attributable to turbulence that affects the observed curve but that is not accounted for in the model.

We checked the reservoir description resulting from the matching procedure by observing that (1) total field gas in place at a prescribed pressure level was in agreement with the observed value, and (2) total field performance against a differential of approximately 10×10^6 psia^2 was close to measured performance. Performance at lower differentials was acknowledged to be slightly conservative.

Well Placement

The 110-day withdrawal season was simulated by the demand vs time schedule as shown in Fig. 3. The schedule was based on three years of history and modified to reflect the desired increased total gas production and last-day deliverability requirement upgraded from 140 to 300 MMcf/D. The general trend of the demand schedule illustrates the unique facet of storage operations: the demand increases as reservoir inventory decreases.

The 38 new wells were originally located in the higher deliverability portion of the reservoir (Fig. 4). All 79 wells were set to flow against a common limiting pressure. The limiting pressure is the bottom-hole equivalent of average gathering line pressure and is found, as shown in Eq. A-34, from

$$\Phi_w = \frac{Q_{\text{demand}} - \sum_{\substack{\text{no.}\\ \text{wells}}} c_{q_{ij}} \Phi_{ij}}{\sum_{\substack{\text{no.}\\ \text{wells}}} c_{q_{ij}}} \quad \ldots\ldots\ldots \quad (3)$$

Using this method, we allowed the line presssure to fluctuate so that the demand was met to within a 2-percent tolerance for each step. A minimum pressure value based on equipment limitations was imposed on the model. When the calculated line pressure hit this minimum, it was held there and the field performance was allowed to decline. With this scheme, the initial 79 well configuration failed to make the required rate on the 107th day of withdrawal, since it could make only 158 of the requested 225 MMcf/D. Results, labeled "Run 1", are shown in Fig. 5.

The 38 new wells were then moved out of the high deliverability region and located in the outer portions of the reservoir to obtain a maximum distance between wells. (See Fig. 6.) Operating in the same manner as Run 1, this run also failed to make the scheduled demand at 107 days,

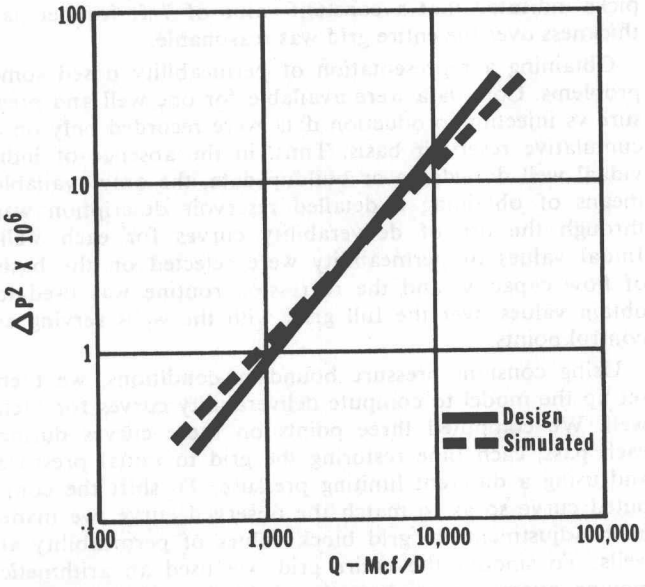

Fig. 2 — *Design and simulated deliverability curves.*

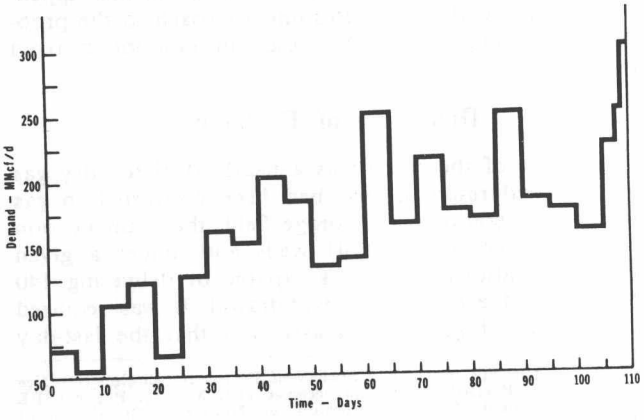

Fig. 3 — *110-day demand schedule.*

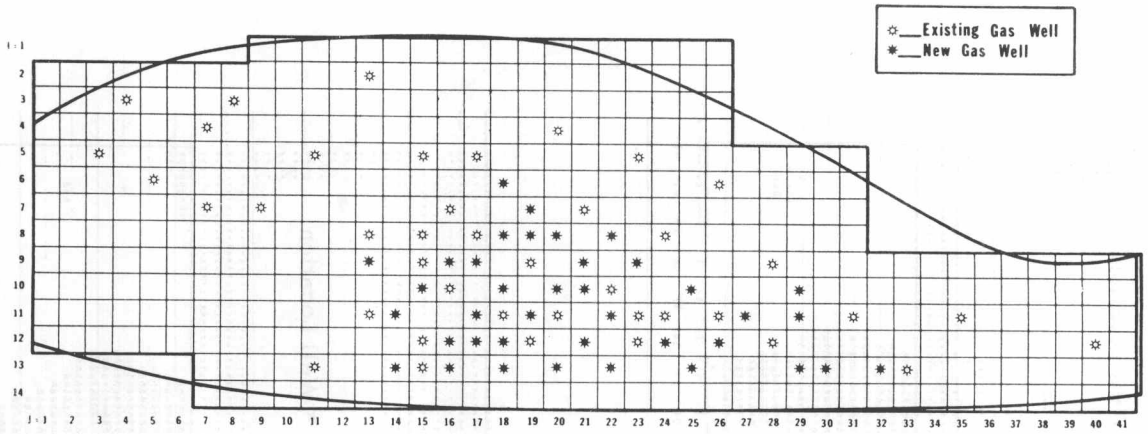

Fig. 4 — *Well locations, Set 1.*

but was able to produce 212 of the requested 225 MMcf/D at the time of failure. The performance of this system is shown as "Run 2" in Fig. 5. Figs. 7 and 8 are maps showing the relative pressure levels at 110 days for the two well patterns. On these maps, an "8" was printed for any pressure between 0.75 and 0.85 times original pressure, a "6" for 0.55 to 0.65 times original pressure, etc. The odd digits were omitted for clarity. Both maps show that the central high deliverability region of the reservoir has been drawn down to low pressures while the outer areas, particularly at the left edge, remain at about 9/10 original pressure.

Variations in Operation

The fact that some areas of the reservoir were being drawn down quite severely while others were virtually unaffected led to the design of a scheme that would permit scheduling of the time when wells were to be made available to the system. Using Well Pattern 2, the wells were listed in order of turn-on, with the perimeter wells first and the high capacity wells last. This order was prompted by the facts that (1) the demand generally increased as the reservoir was depleted during the season, and (2) at the latter part of the season we had not drawn as much gas from the tighter sections of the reservoir while the high capacity portion was down to approximately 40 percent of original pressure. The objective, therefore, was to force the "poorer" wells to produce as much gas as possible; this would insure drainage of the outer areas of the reservoir and allow the better quality wells to rest until needed for meeting demand peaks. To accomplish this, the

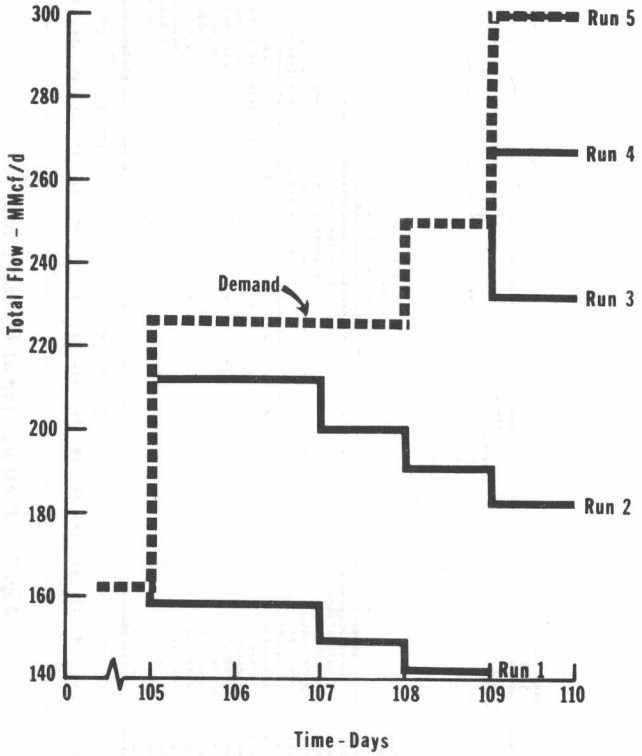

Fig. 5 — *Demand vs performance, 105 to 110 days.*

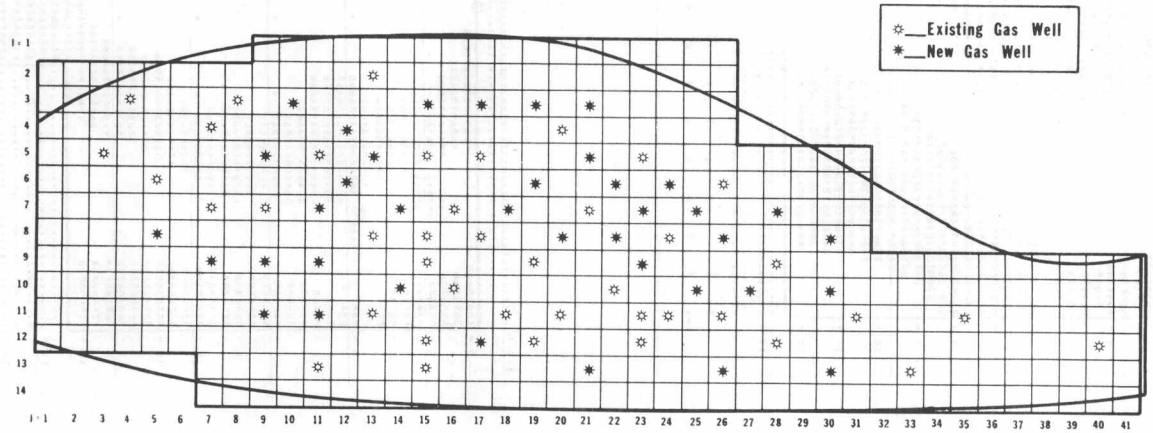

Fig. 6 — *Well locations, Set 2.*

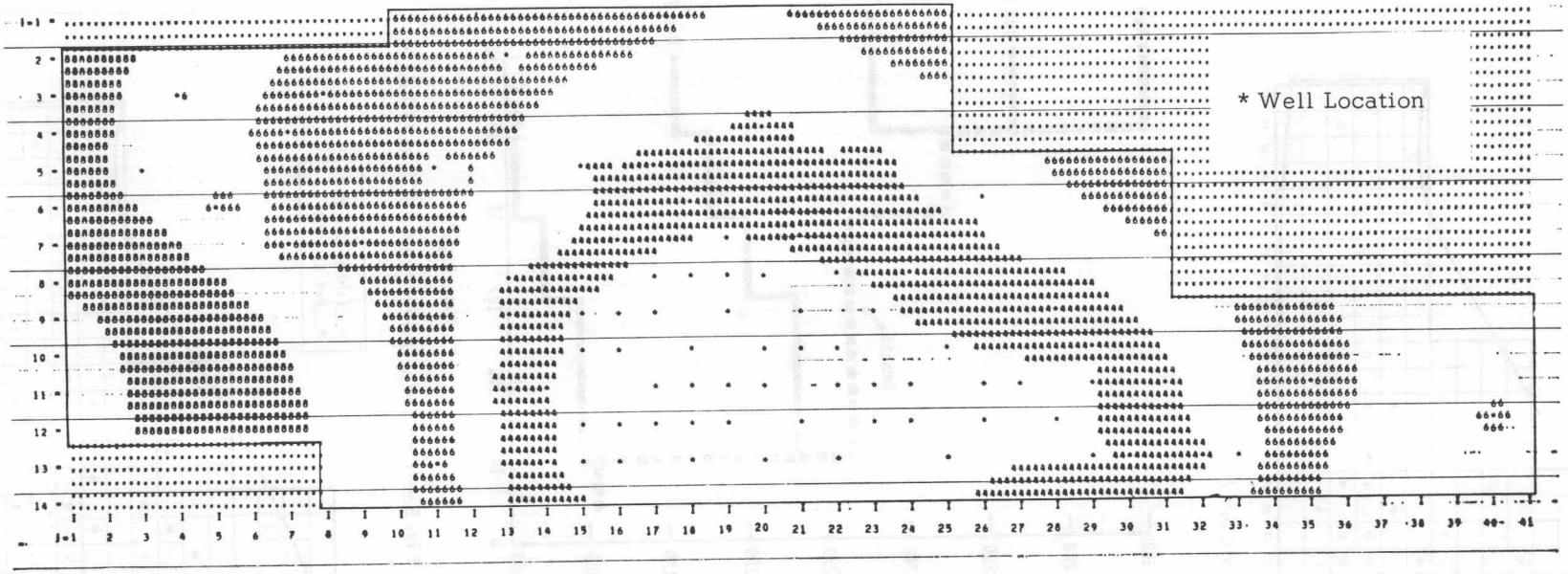

Fig. 7 — *Pressure map at 110 days, Run 1.*

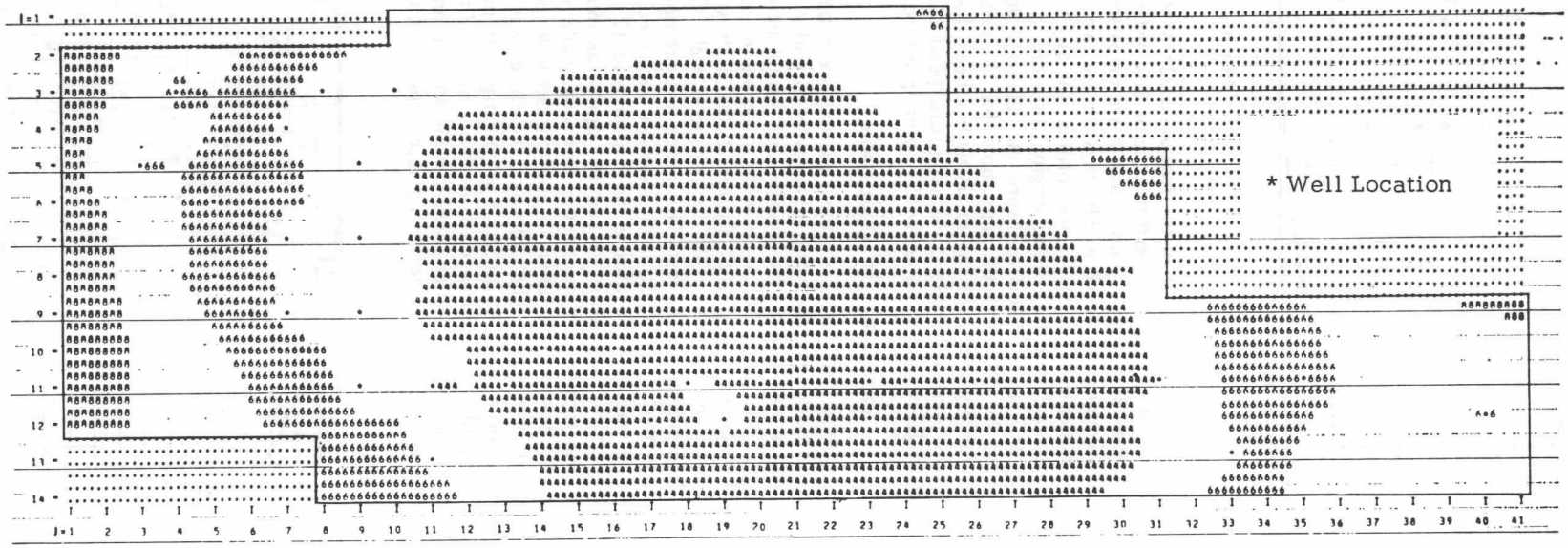

Fig. 8 — *Pressure map at 110 days, Run 2.*

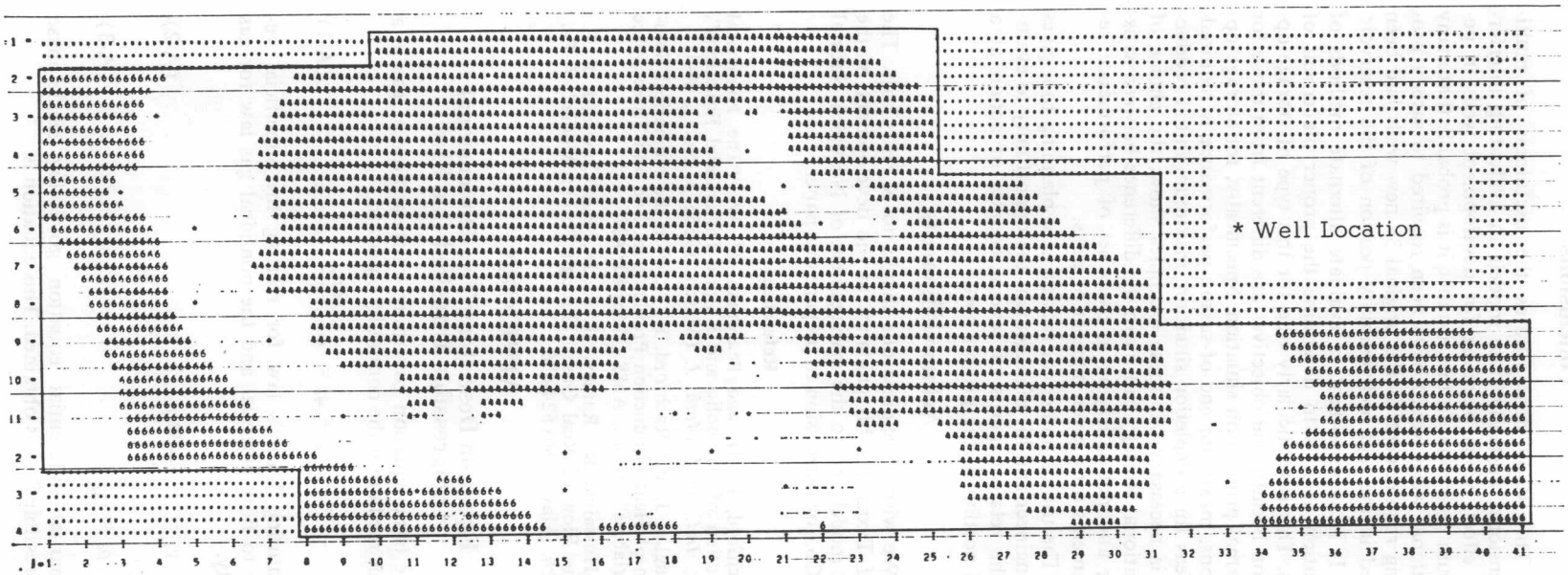

Fig. 9 — *Pressure map at 110 days, Run 3.*

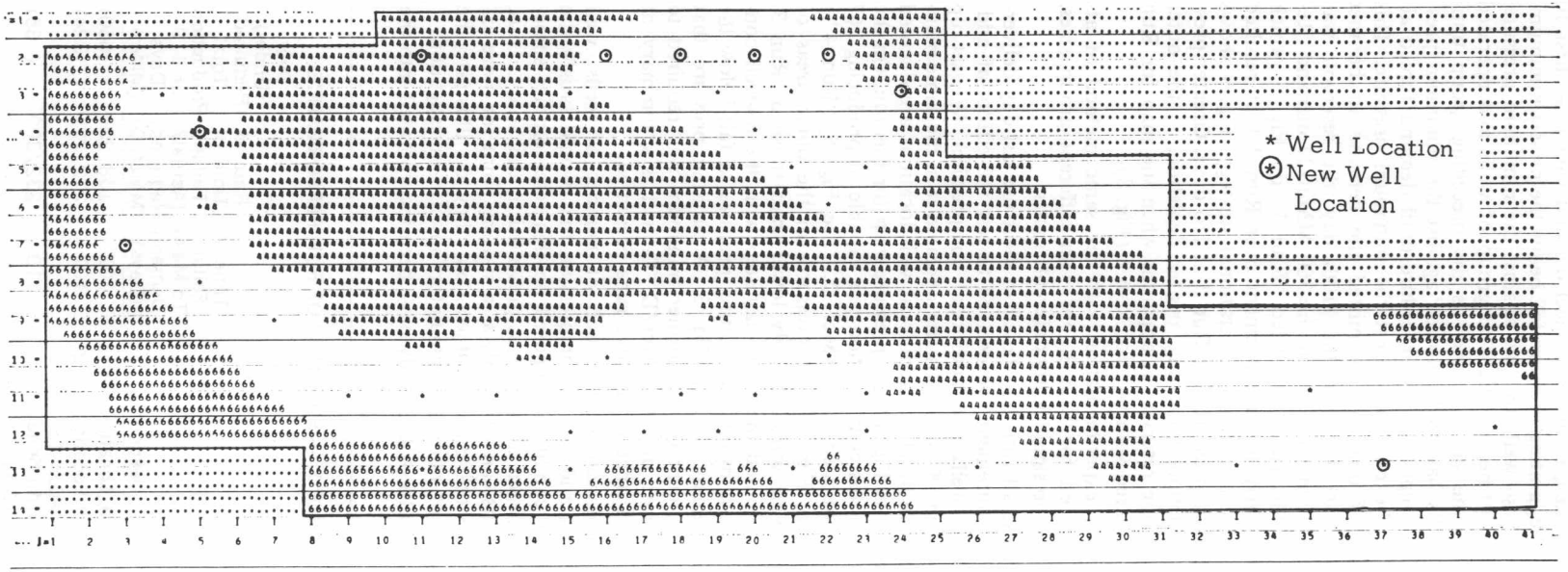

Fig. 10 — *Pressure map at 110 days, Run 4.*

well schedule was divided into groups of 10 wells each, with 9 wells making up the last group. We started the run by flowing only the first group (composed of perimeter wells) against a common limiting pressure as calculated by Eq. 3. When, in order to meet demand with these first 10 wells, the limiting pressure fell below the pre-set minimum, we set these wells to flow against the minimum pressure. We then turned on the next group of wells and operated them in the same manner as the preceding group until these wells had to be flowed against the minimum pressure. We repeated this procedure until demand forced all wells to be on line against the minimum pressure. This method of operation permitted the demand to be met through 109 days. On the 110th day, the reservoir was capable of making 232 of the 300 MMcf/D demand. Results of this run are labeled "Run 3" on Fig. 5, which shows clearly the improvement over Run 2 that resulted from only a change in operational strategy. Fig. 9 shows the relative pressures for Run 3 at 110 days. Greater pressure reduction, indicating greater depletion, in the outer areas of the reservoir is apparent when the map for Run 3 is compared with that for Run 2 (Fig. 8).

Further experimentation with the same method of attack as used for Run 3, but with different group sizes, produced no significantly different results.

Because all runs had failed to meet the last-day deliverability requirement, we decided to test the effects of adding more wells and additional compression. We set up Run 4 with 88 total wells and operated it in the same manner as Run 3. The 9 additional well locations are denoted by circles on Fig. 10, the pressure map for this run. On the 110th day this configuration was capable of producing 267 of the requested 300 MMcf/D. (See Fig. 5, "Run 4".) Note from Fig. 10 that pressures in the outer areas of the reservoir were generally lower than those of Run 3. We recomputed the 110th-day step with the 88-well configuration, allowing the limiting pressure to fall below the former minimum using Eq. 3. A limiting pressure that was 80 percent of the former minimum was required to obtain a rate of 300 MMcf/D. Table 1 is a summary of the performance of the five runs presented.

The optimum combination of number of wells, well placement and use of compression that would satisfy the particular conditions imposed on this reservoir lies somewhere between the extremes presented in this study. Thus, these results can serve only as a starting point for more exhaustive work on the subject, but they do illustrate the flexibility of numerical simulators in such investigations.

The results of this study have been incorporated into the field operations to deal with problems of new well placement and have been applied to the production-injection strategy as discussed here.

TABLE 1 — SUMMARY OF RUN PERFORMANCE

Run	Description	Time of Failure To Make Demand (Days)	Rate at Time of Failure [Actual/ Required] (MMcf/D)	Over (Under) Required Total Production at 110 Days (MMcf)
1	Well Location Set 1	107	158/225	(660)
2	Well Location Set 2	107	212/225	(324)
3	Location Set 2 — With Scheduling	110	232/300	(65)
4	Run 3 Plus Nine Additional Wells	110	267/300	(14)
5	Run 4 With Additional Compression On Last Day	No Failure	———	19

Conclusions

1. This study demonstrates the usefulness of multidimensional unsteady state models in evaluating interference effects when planning for development wells in petroleum reservoirs. In this instance it is probable that many additional wells would have been required to satisfy producing requirements if the original 38 new wells had been placed in the high deliverability portion of the reservoir.

2. It is as important to evaluate alternate methods of operation as it is to determine the proper placement of wells. This is particularly true for this type of storage operation because the objectives are different from those for a normal production situation. Specifically, for storage operations, maximum end-of-season performance is required, whereas for a depletion situation, maximum initial production is necessary. As these examples show, the choice of operational strategy can mean the difference between satisfying and not satisfying a given set of performance requirements for a given number of wells.

3. The use of numerical models as a planning tool gives the engineer and his management the opportunity to evaluate the relative merits of several courses of action at a small portion of the project cost.

Acknowledgments

We wish to express our thanks to K. H. Coats, The U. of Texas, for his guidance in the development of the basic model and to the management of Northern Natural Gas Co. for permission to prepare this paper.

References

1. Rachford, H. H. and Peaceman, D. W.: "The Numerical Solution of Parabolic and Elliptic Differential Equations", *Soc. Ind. Appl. Math. J.* (March, 1955) **3,** No. 1, 28-41.

2. Douglas, J. and Rachford, H. H., "On the Numerical Solution of Heat Conduction Problems in Two and Three Space Variables", *Trans.*, AMS (1956) **82,** 421.

3. Al-Hussainy, R., Ramey, H. J., Jr., and Crawford, P. B.: "The Flow of Real Gases Through Porous Media", *J. Pet. Tech.* (May, 1966) 624-636.

APPENDIX

Equation Describing Two-Dimensional Compressible Transient Gas Flow

The basic equation governing transient flow of gas in a porous medium is the continuity equation,

$$-\nabla \cdot \rho_g v_g + q_g = \phi S_g \frac{\partial \rho_g}{\partial t} \quad . \quad . \quad . \quad . \quad . \quad . \quad . \quad (A\text{-}1)$$

Substituting Darcy's law for relating the superficial velocity to flow potential and the non-ideal gas law for gas density,

$$v_g = -\frac{k}{\mu} \nabla p \quad , \quad . \quad . \quad . \quad . \quad . \quad . \quad . \quad . \quad . \quad (A\text{-}2)$$

$$\rho_g = \frac{p}{zRT} \quad , \quad . \quad . \quad . \quad . \quad . \quad . \quad . \quad . \quad . \quad (A\text{-}3)$$

the partial differential equation governing single-phase compressible flow is obtained. This equation is

$$\nabla \cdot k \nabla \Phi + q_g = \phi S_g \frac{\partial \frac{p}{z}}{\partial t} \quad , \quad . \quad . \quad . \quad . \quad . \quad . \quad (A\text{-}4)$$

where

$$\Phi = \int_o^p \frac{p}{z(p)\mu(p)} dp \text{ (real gas potential)} \quad \text{(A-5)}$$

Using the relationship

$$\frac{\partial \frac{p}{z}}{\partial t} = \frac{d\frac{p}{z}}{d\Phi}\frac{\partial \Phi}{\partial t} \quad \text{(A-6)}$$

to alter the right-hand side of Eq. A-4, the diffusivity equation for single phase flow of gas in terms of the flow potential Φ is

$$\nabla \cdot k \nabla \Phi + q_v = \phi S_g C' \frac{\partial \Phi}{\partial t}, \quad \text{(A-7)}$$

where

$$C' = \frac{d\frac{p}{z}}{d\Phi} \quad \text{(A-8)}$$

Through this transformation we have eliminated all pressure-sensitive components of the coefficients of the space derivatives.

Expressing Eq. A-7 in difference form and multiplying by the block volume ($h\Delta x\Delta y$) gives Eq. A-9.

$$\Delta A \Delta \Phi + Q = PV C' \Delta_t \Phi, \quad \text{(A-9)}$$

where:

$$\Delta A \Delta \Phi = \Delta_x AX \Delta_x \Phi + \Delta_y AY \Delta_y \Phi, \quad \text{(A-10)}$$

$$\Delta_x AX \Delta_x \Phi = AX_{i+\frac{1}{2},j}(\Phi_{i+1,j} - \Phi_{i,j}) - AX_{i-\frac{1}{2},j}(\Phi_{i,j} - \Phi_{i-1,j}), \quad \text{(A-11)}$$

$$AX_{i+\frac{1}{2},j} = \left(\frac{kh\,\Delta y}{\Delta x}\right)_{i+\frac{1}{2},j}, \quad \text{(A-12)}$$

$$C' = \frac{\left(\frac{p}{z}\right)^k - \left(\frac{p}{z}\right)^n}{\Phi^k - \Phi^n}, \quad \text{(A-13)}$$

$$PV = (h\phi S_g \Delta x \Delta y), \quad \text{(A-14)}$$

$$\Delta_t \Phi = \frac{\Phi^{n+1}_{i,j} - \Phi^n_{i,j}}{\Delta t}, \quad \text{(A-15)}$$

and $x = i\Delta x$, $y = j\Delta y$, $t = n\Delta t$.

To express Eq. A-9 in a form suitable for solving with the ADI technique, Eqs. A-16 and A-17 are superscripted for the iteration process (k denotes the k^{th} iterate) and an acceleration parameter, $\overline{H}_k$, is added to each equation.

$$\Delta_x AX\Delta_x\Phi^{k+1} + \Delta_y AY\Delta_y\Phi^k + c_q(\Phi_w - \Phi^{k+1}) = PV C'^k(\Phi^{k+1} - \Phi^n) + \overline{H}_k(\Phi^{k+1} - \Phi^k), \quad \text{(A-16)}$$

$$\Delta_x AX\Delta\Phi^{k+1} + \Delta_y AY\Delta_y\Phi^{k+2} + c_q(\Phi_w - \Phi^{k+2}) = PV C'^k(\Phi^{k+2} - \Phi^n) + \overline{H}_k(\Phi^{k+2} - \Phi^{k+1}), \quad \text{(A-17)}$$

where:

$$\overline{H}_k = H_k \Sigma A, \quad \text{(A-18)}$$

and

$$c_q = \frac{\alpha 2\pi hkT_{sc}}{\left(\ln\frac{r_e}{r_w} - \frac{1}{2}\right)T_R p_{sc}} \quad \text{(A-19)}$$

Define

$$\Phi X = \Phi^{k+1} - \Phi^k \quad \text{(A-20)}$$

and

$$\Phi Y = \Phi^{k+2} - \Phi^k \quad \text{(A-21)}$$

Using these definitions, substraction of Eq. A-17 from Eq. A-16 and rearrangement of the results yields the following equations used for the x and y calculations, respectively.

$$\Delta_x AX\Delta_x \Phi X - (c_q + \overline{H}_k + PV C'^k)\Phi X = PV C'^k(\Phi^k - \Phi^n) - c_q(\Phi^k - \Phi_w) - \Delta A\Delta\Phi^k, \quad \text{(A-22)}$$

$$\Delta_y AY\Delta_y \Phi Y - (c_q + \overline{H}_k + PV C'^k)\Phi Y = -(c_q + 2\overline{H}_k + PV C'^k)\Phi X \quad \text{(A-23)}$$

The standard ADI technique[1,2] is then invoked on Eqs. A-22 and A-23 to solve the system.

Implicit Production - Injection Technique

To approximate wellbore conditions realistically, we developed a technique that assumes Darcy flow in the block in which a well is located. The technique outlined here is designed for use in implicit models that have as the dependent variable the integral transform or fluid potential.

Darcy's law for radial gas flow, transformed to standard conditions, is

$$q_{sc} = \frac{\alpha 2\pi rhkpT_{sc}}{\mu z T_R p_{sc}}\frac{dp}{dr}. \quad \text{(A-24)}$$

Defining the "real gas potential"[3] as the integral Φ,

$$\Phi = \int_o^p \frac{p}{z(p)\mu(p)} dp, \quad \text{(A-25)}$$

and substituting Eq. A-25 into Eq. A-24 yields

$$q_{sc} = \frac{\alpha 2\pi\, rhkT_{sc}}{T_R p_{sc}}\frac{d\Phi}{dr} \quad \text{(A-26)}$$

Factoring Eq. A-26 gives the integral equation

$$\int_{r_w}^{r} \frac{q_{sc}T_R p_{sc}}{\alpha 2\pi hkT_{sc}}\frac{dr}{r} = \int_{r_w}^{r} d\Phi. \quad \text{(A-27)}$$

Letting

$$\hat{q} = \frac{q_{sc}T_R p_{sc}}{\alpha 2\pi hkT_{sc}}, \quad \text{(A-28)}$$

substituting Eq. A-28 into Eq. A-27, and integrating both sides yields

$$\hat{q}\ln\frac{r_w}{r} = \Phi(r) - \Phi_w \quad \text{(A-29)}$$

Defining a $\overline{\Phi}$, which is the integrated average potential bounded by the volume computed for some external radius, r_e,

$$\overline{\Phi} = \frac{\int_{r_w}^{r_e}\Phi(r)2\pi r\, dr}{\pi r_e^2}, \quad \text{(A-30)}$$

solving Eq. A-29 for $\Phi(r)$, and substituting into Eq. A-30 yields

$$\bar{\Phi} = \frac{2}{r_e^2}\int_{r_w}^{r_e}\left(\Phi_w - \hat{q}\ln\frac{r}{r_w}\right) r\,dr \quad . \quad . \quad . \quad \text{(A-31)}$$

Carrying out the integration indicated in Eq. A-31 and neglecting the r_w^2 terms that appear as multipliers gives

$$\bar{\Phi} = \Phi_w + \hat{q}\left(\ln\frac{r_e}{r_w} - \frac{1}{2}\right) \quad . \quad . \quad . \quad . \quad . \quad . \quad \text{(A-32)}$$

Assuming steady state flow in the block in which a well is located, Eqs. A-28 and A-32 can be combined to obtain

$$q_{sc} = \frac{\alpha 2\pi\, hkT_{sc}}{\left(\ln\frac{r_e}{r_w} - \frac{1}{2}\right)T_R\, p_{sc}}(\bar{\Phi} - \Phi_w) \quad , \quad . \quad \text{(A-33)}$$

where

$\bar{\Phi}$ is the block calculated potential,

Φ_w is the potential at the well,

r_e is equal to $\Delta x/2$ in the case of $\Delta x = \Delta y$,

and $\sqrt{\frac{\Delta x \Delta y}{\pi}}$ for $\Delta x \neq \Delta y$

α is the conversion constant for field units equal to 6.328×10^{-3} for k in millidarcies, and q_{sc} in Mscf/D, and h is the thickness of the well block in feet.

Constant Terminal Pressure Condition

In this case Φ_w is specified as the known condition and a q_{sc} is then calculated from the resulting $\bar{\Phi}$ in the well block for a particular time step.

Constant Terminal Rate Condition

In this case Φ_w is assumed and iterations are performed until the q_{sc} calculated from Eq. A-33 closes on a desired rate. On each iteration Φ_w is corrected by the following relationship.

$$\Phi_w{}^k = \Phi - \frac{q_{sc}\left(\ln\frac{r_e}{r_w} - \frac{1}{2}\right)T_R \quad p_{sc}}{\alpha 2\pi\, hkT_{sc}}, \quad . \quad . \quad \text{(A-34)}$$

where q_{sc} in Eq. A-34 is the desired rate for this boundary condition and the rest of the terms are as given by Eq. A-33. In the case of multi-wells, all subscripted terms are involved in summations.

Incremental Material Balance

The test for closure used for this system was a check on the incremental mass balance over a time step. The relationship used is given by Eq. A-35.

$$\left|\frac{\sum_{i,j} PV\, C'^k\,(\Phi^{k+2} - \Phi^n) - \sum_{\substack{\text{no.}\\ \text{wells}}} c_q\,(\Phi_w - \Phi^{k+2})}{\sum_{\substack{\text{no.}\\ \text{wells}}} c_q\,(\Phi_w - \Phi^{k+2})}\right| < \varepsilon \quad \text{(A-35)}$$

where ε is some small acceptable error. ★★★

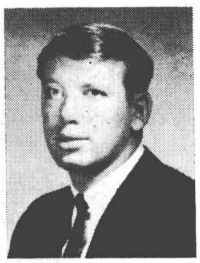

James C. Tyler *is a scientific analyst for Northern Natural Gas Co. in Omaha. Tyler graduated from the U. of Nebraska in 1966 with degrees in mathematics and physics. Biographical sketches and pictures of* **J. H. Henderson** *and* **J. R. Dempsey** *can be found on Page 1132 of the Oct., 1968, issue of* JOURNAL OF PETROLEUM TECHNOLOGY.

Use of Injection-Falloff Tests To Evaluate Storage Reservoirs

G. A. Mistrot, SPE-AIME, Southern Natural Gas Co.
J. R. Dempsey, SPE-AIME, INTERCOMP Resource Development and Engineering Inc.
Richard W. Snyder, SPE-AIME, INTERCOMP Resource Development and Engineering Inc.

Introduction

Probably the single most important piece of reservoir data required in the conversion of a depleted gas field to gas storage service is effective rock permeability distribution, and this information is usually not available in sufficient detail during the primary depletion of the field. Wells are drilled on relatively wide spacing; and core or buildup data, even where available, provide insufficient points of control for adequate mapping. Matching history with a reservoir simulator can sometimes fill in the gaps, but it is not uncommon for areal history matches to be somewhat insensitive to relatively wide variations in over-all reservoir permeability and individual well descriptive parameters (such as damage, turbulence, and crossflow) at the producing rates at which the field was depleted.

As the field is being converted to storage mode, infill drilling provides the required additional points of control. Normally, good porosity limits can be obtained through logging programs, but permeability is another matter.

Drilling into pressure-depleted reservoirs with gas- or nitrogen-lightened mud is often ruled out from a cost standpoint, and deep invasion is commonplace when nonaerated muds are used. Additionally, costs in general and costs and problems resulting from lost circulation usually preclude extensive coring.

Completed wells more often than not have significant damage and insufficient pressure to flow out invaded fluids and produce at rates and pressures that will permit an acceptable evaluation. In addition to filtrate invasion, it is not uncommon for some solids to drop out, completely blocking the sand face and requiring the well to be acidized before it will even accept gas on injection. Acidizing — even a small job — is at best a necessary evil as it adds more liquids to an already invaded zone. Deep and severe damage can affect pressure transients for a substantial period of time.

A testing method must be designed that can yield usable information even at low rates and in severely damaged environments. The analytical technique must be able to provide the following:

1. Extent of damage;
2. Permeability of the undamaged zone;
3. Effect or significance of geological heterogeneity;
4. Predicted injectivity capability, including the effects on injectivity resulting from the removal of damage or from the eventual perforation of a previously unperforated productive interval;
5. Degree of reliability of test analysis and interpretation.

If the field data are taken carefully, their trend should be valid, and the results of a test should be accurate within plus or minus a specific and determinable percentage.

Injection-falloff tests provide a relatively inexpensive means of obtaining information from which adequate analyses can be made. One or more of the original wells can usually be used as a gas source,

Injection-falloff tests are useful during the conversion of a depleted field into a gas storage system. When production testing is not possible, injection-falloff testing can provide the essential data, and an analysis of them can yield acceptable values of permeability and degree of wellbore damage.

and the gas can be compressed with either an existing machine or a portable single-stage field compressor. The test procedure described in this paper consists of one or more injection periods, at different rates, each followed by a falloff. This approach differs from those previously described in that four or more separate unsteady-state pressure-time sequences are analyzed for near-wellbore effects and formation permeability. This approach of alternating injection and shut-in maximizes the transient effects and makes an adequate history match more difficult, but once accomplished, more dependable. The number of different rates at which a well is tested, and the length of each injection and falloff period will depend on the characteristics of the reservoir and the individual well. Often a two-rate test that can be completed in one working day is sufficient.

Test Procedures

In the field from which the examples were taken, test gas was produced from one of the original wells and compressed in a 100-hp single-stage portable machine capable of discharging about 1,300 Mcf/D at approximately 800 psig.

After long string is set on a well, mud is displaced with water, a permanent packer is set about 50 ft above the producing zone, tubing is run, and the tree is set. The well is swabbed to the top of the packer, logged and perforated, and injection is begun. If necessary, the well is acidized, and it is injected into at the maximum attainable rate for several days to move the invaded fluids as far away from the wellbore as possible. Injection pressures during this initial cleanup period decline substantially. At such time as injection pressure has fairly well leveled off — generally after 3 days to 1 week — the well is shut in for 2 hours, then tested in the following sequence:

1. Three-hour injection at low rate,
2. Two-hour falloff,
3. Three-hour injection at high rate,
4. Overnight falloff.

Tubing pressure is deadweighted at regular intervals throughout the test.

It is not uncommon for a well to continue to clean up during the test, and running the test at a low rate first permits the cleanup effect to be isolated rather than mistaken for a change in turbulence, which could happen if the test were run at a high rate first. Conversely, an apparent increase in damage during the test would be an indication of significant turbulence. The characteristic of gas wells' cleaning up with throughput and the problems this causes in test interpretation have been discussed in the literature.[1-3]

Test rates selected were 600 to 700 Mcf/D for the low rate, and maximum attainable for the high rate. At these rates, volume injected is negligible compared with gas in place in the segment of the reservoir seen by the pressure transient, so the test is quite insensitive to gross section porosity, being affected by permeability variations only.

Six of the original wells and two new storage wells were cored, and the analyses were used to develop correlations for the range of permeability to be expected for any given value of porosity.

Porosities calculated from logs, and permeabilities read from the above-mentioned correlations, were used to provide the initial reservoir description for history-matching the tests in an unsteady-state gas model with r-z geometry.[4] History match is effected by holding the porosity constant and changing the permeability by multipliers, essentially keeping, where possible, the same slope of the porosity/permeability relationship. In any event, the permeability assigned to an interval was kept within the range or band of values that core data indicated could be expected for the log-derived porosity for that interval.

The final reservoir descriptions showed permeability variations from layer to layer, which on the face of it, suggests unique solutions. Such an implication is not intended. Once an acceptable match was obtained, individual layer properties were varied over a wide range, and the accepted description was the one giving the best fit of the data.

The analytical procedure is aimed at obtaining results that are accurate within acceptable engineering tolerances, and the tests were modeled so that matched properties could be varied to test the degree of dependability of the results and the corresponding effect on predictions. If the best history match is questionable, or if it points to some anomalous conditions, a second test, based on the results of the first, can be designed to investigate the problem.

For the times used, the transient is generally seen to 250 ft and occasionally as far as 500 ft from the wellbore, roughly one-fourth to a maximum of one-half the well spacing. These particular tests, then, were not designed to necessarily yield "average drainage radius" permeabilities, but rather, to yield essentially point data that are contoured to develop the permeability distribution for the field. The reservoir rock is a clean, well consolidated, fine-to medium-grain sandstone, and permeability variations from well to well are not extreme. The permeability map was entered in a multidimensional reservoir simulator to make fieldwide predictions and quantitative estimates of individual well performance.

Field Example 1

The well penetrated 78 ft of productive section, leaving an estimated 20 ft between the bottom of the well and the gas/water contact. Fig. 1 depicts the final matched reservoir description and completion intervals. Other parameters are as follows:

Total depth, ft	5,550
Reservoir pressure in vicinity of well, psia	628
Reservoir temperature, °R	590
Gas gravity	0.66
Long string	7⅝ in. set in 9⅞-in. hole
Tubing ID, in.	3½
Packer set, depth in ft	5,308

The well was swabbed down to the packer, perforated, acidized with 3,000 gal of mud acid, and injected into for 6 days at an average rate of 1,300 Mcf/D, during which time injection pressure declined from 865 to 729 psia.